The SAS-3 X-Ray Observatory

by
W. F. Mayer

The SAS-3 satellite consists of an experiment section, built by MIT, and an improved version of the SAS spacecraft, built by APL. The spacecraft improvements provide the flexibility needed to operate the SAS-3 payload in near real-time as an X-ray observatory. Brief descriptions of five observations are presented to illustrate the use of the spacecraft in scientific investigations.

Introduction

The SAS-3 satellite is an X-ray observatory with three major objectives: to determine the location of bright X-ray sources to an accuracy of 15 arc-seconds; to study a selected set of sources over a wide energy range, from 0.1 to 55 keV; and to search the sky continuously for X-ray novae, flares, and unexpected phenomena. The scientific portion of the observatory was designed and built for NASA by the Laboratory for Space Experiments and the Center for Space Research of M.I.T. (Massachusetts Institute of Technology). The scientific experiment was mated with a spacecraft designed and built at APL, to form the SAS-3 payload (Explorer 53).

The field of X-ray astronomy originated in 1962 with the first detection of a celestial (nonsolar) X-ray source during a sounding rocket flight that was primarily designed to detect solar X-rays that fluoresced from the moon's surface. Since then, X-ray astronomy has expanded rapidly as a result of data obtained from sounding rocket and balloon flights and from X-ray experiments on OSO-7, SAS-1 and -2, UK-5, and the ANS satellites.

At the time of the SAS-3 launch in May 1975, about 200 celestial X-ray sources had been detected. About 30 of them have been identified with optical or radio objects. Among the 30, there are several distinct classes of objects. Some X-ray emitters within our galaxy are large stellar remnants from supernova explosions (e.g., the Crab Nebula, which exploded in 1054 A.D.). Examples of other types of X-ray sources include a mysterious region 10^3 light-years in diameter located at the center of our galaxy, and binary star systems comprising an ordinary star with a radius of more than 10^9 m and a nearby superdense companion (a neutron star, black hole, or white dwarf).

Outside our galaxy the diversity is even greater: quasars; Seyfert galaxies that contain very active nuclei; radio galaxies; and vast regions that extend over several million light-years at the centers of rich clusters of galaxies and contain several hundred galaxies.

Figure 1 is a plot of the X-ray sky in galactic coordinates (ℓ^{II} and b^{II}); the horizontal axis is the plane of the Milky Way Galaxy. Coma and Virgo are rich clusters of galaxies. The Large (LMC) and Small (SMC) Magellanic Clouds and M31 are single galaxies; 3C273 is a quasar. Cygnus A (CYG A) is a giant radio-emitting galaxy that also emits X rays. Scorpius X-1 (SCO X-1) has been identified with a blue flickering star that has many of the characteristics of an old nova. Hercules X-1 (Her X-1), Centaurus X-3 (Cen X-3), Vela X-1, and Cygnus X-1 (Cyg X-1) are binary star systems that include a normal though massive star and a small, superdense companion, now believed to be either a neutron star (Her X-1, Cen X-3 and Vela X-1) or possibly a black hole (Cyg X-1). NGC 1275 is a bright exploding radio galaxy. The Crab Nebula is the remnant of a supernova explosion that occurred 922 years ago.

With this vast amount of information already known, the SAS-3 experiment and spacecraft were designed for a second generation of X-ray measurements. In contrast with the earlier survey satellites, SAS-3 was designed to perform very specific measurements of the position, spectra, and time variability of known X-ray sources, while monitoring the sky for new X-ray novae. M.I.T., APL, and Goddard Space Flight Center (GSFC) of NASA worked together to produce an experiment and spacecraft capable of meeting these goals.

The improvements in APL's SAS-3 spacecraft include a clock accurate to 1 part in 10^{10}, rotatable solar panels, a programmable data format, an improved nutation damper, a delayed command sys-

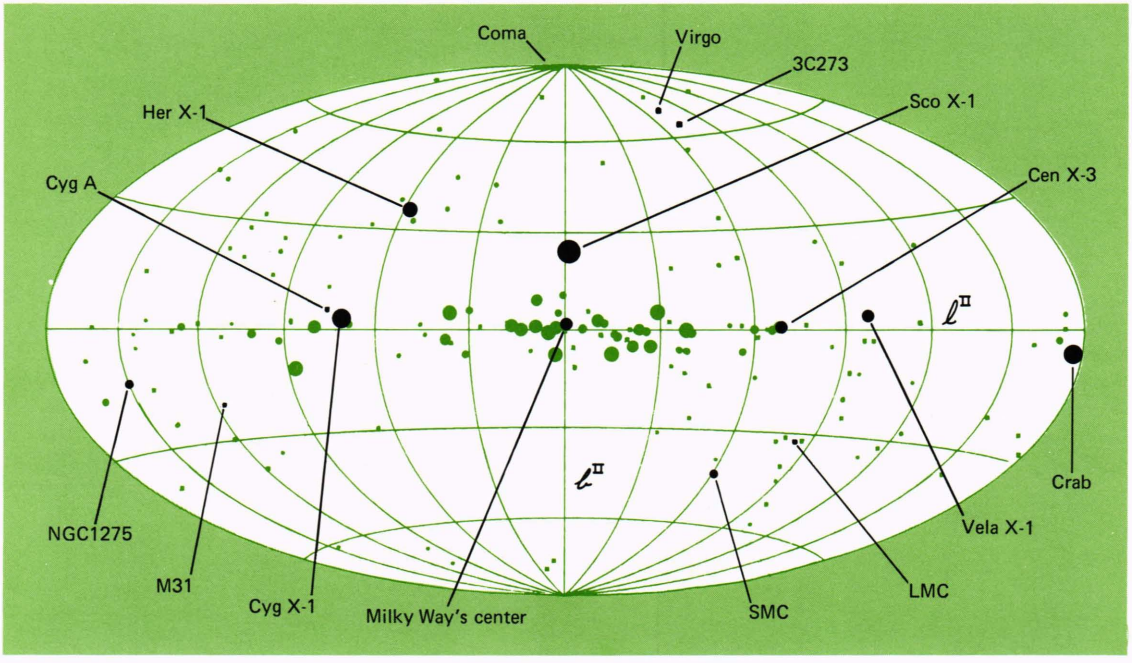

Fig. 1—The X-ray sky. The positions of some of the known X-ray sources are plotted in galactic coordinates. The horizontal axis is the plane of the Milky Way Galaxy with the galactic center at the middle of the plot. The sizes of the blackened circles are roughly proportional to the observed intensity of the sources in the energy range of 2 to 10 keV.

tem, an improved magnetic trim system, and an azimuth control system using a variable-speed angular momentum wheel in a closed loop feedback system with a commandable rate gyro. They enable us to operate the SAS-3 satellite as a true observatory, since we can perform three-axis stabilized observations of any point on the celestial sphere at any time of the year. The significance of the improvements can be seen in the following descriptions of the experiment section, the SAS-3 operations, and brief synopses of a few experimental observations.

Experiment Description

The experiment section of the SAS-3 observatory includes a number of X-ray and optical detector systems, each designed to accomplish one of the scientific goals, and the associated electronic, mechanical, and thermal control systems necessary to operate these primary detectors. Each X-ray detector system consists of one or more proportional counters, similar to Geiger tubes, that convert incident X rays into low-level electrical signals. The region of the sky seen by each proportional counter is defined by a collimator appropriate to the measurement involved. The optical detectors on the experiment are used to determine the precise orientation (aspect) of the satellite so that the data from the X-ray detector systems can be correlated with the optical sky.

Figure 2 is a schematic drawing of the SAS-3 experiment. The top view shows the location of an electronic star camera (which is an aspect sensor) and two modulation collimators that have view directions parallel to the satellite spin axis (Z axis). The modulation collimators have angular resolutions of 2.3 and 4.5 arc-minutes and overall fields of view of 12°. The star camera provides the two-dimensional positions of stars brighter than 7th magnitude within an $8° \times 8°$ field of view. The modulation collimators and star cameras enable us to determine the positions of X-ray sources to about 10 arc-seconds after corrections have been made for optical and electronic distortions, temperature variations, magnetic field strength, and star intensity effects.

In the front view of Fig. 2, one can see a three-section slat collimator used in the sky monitoring experiment (SME). The three collimators define long narrow fields of view centered on the satellite Y axis. The field of view of the center slat has angular dimensions of $1° \times 30°$ and is oriented in the Y,Z plane of the satellite. The fields of view of the left and right slat collimators have angular

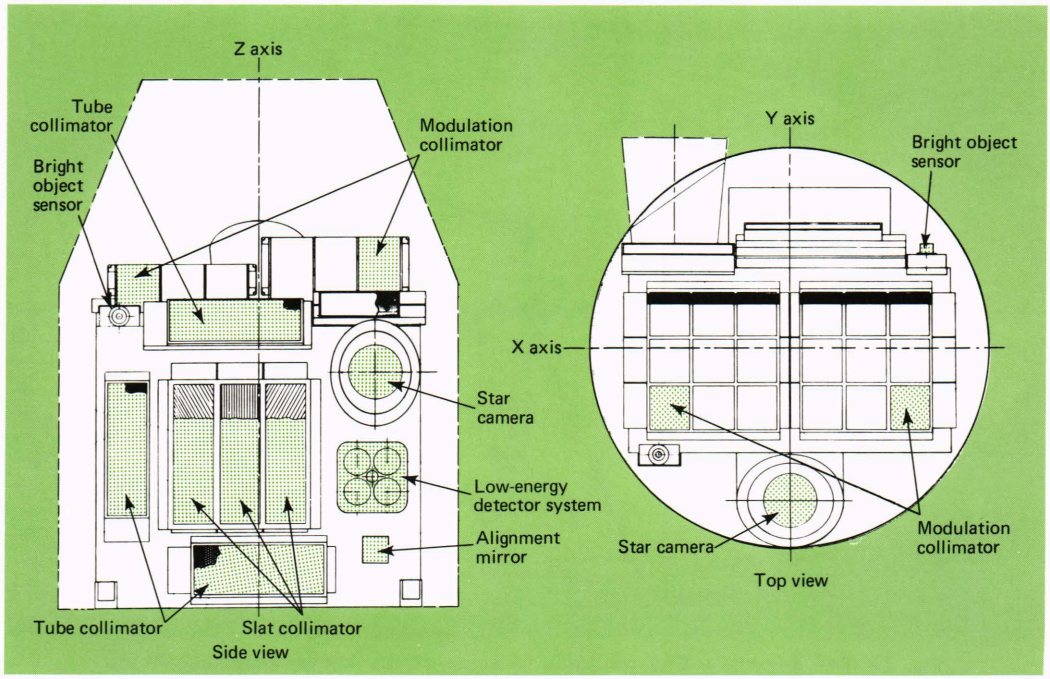

Fig. 2—Schematic drawing of the SAS-3 experiment. The right portion is a top view (Z axis) of the experiment; the left portion is a front view (Y axis). The experiment-to-spacecraft interface is at the bottom of the experiment. Since all non-Z-axis detectors are on the front of the experiment, earth occultation can be avoided by synchronizing the spin rate with the orbital period of the satellite.

dimensions of 0.5° × 32°; they are inclined 30° to the left and right of the Y,Z plane. The long fields of view of these detector systems provide coverage of about half the sky during each revolution of the satellite. In addition, the position of any source can be determined to about 1° by mapping on the sky the field of view of each collimator at the time the source is detected in the collimator. The area of the sky common to all three fields of view must then contain the X-ray source.

Another star camera that views along the main X-ray view direction (Y axis) and a low-energy detector system are to the right of the slat collimators. The low-energy system consists of a set of four grazing-incidence, parabolic reflection concentrators with two independent gas-flow counters sensitive to X rays from 0.15 to 1.0 keV. In order to detect X rays in that energy range, the entrance windows of the proportional counters are made of 0.00004-inch polypropylene. The windows are so thin that the propane gas in the counter diffuses through them; therefore a gas replenishment system is required to maintain a constant pressure in the counter. A filter wheel can be positioned to place any one of five different narrow bandpass X-ray filters simultaneously in the four converging beams from the concentrators.

Above, below, and to the left of the slat collimators are tube collimators that define 1.7° circular fields of view. The proportional counters used in the three systems have various types of windows and gas mixtures to detect X rays from 0.4 to 55 keV. The tube collimator above the slat collimators is inclined at an angle of 5° above the Y axis and therefore can be used as a background reference for the other tube collimators that view along the Y axis.

In addition to the standard electronics associated with each detector system, the experiment also includes a 16-channel pulse height analyzer that can sample the output of any commanded counter to obtain a higher energy resolution of the X rays detected by that counter. There is also a high-speed event monitor that can be used to measure the time variations of the counting rates from selected detectors with time resolutions of 0.12, 1.0, or 8 ms.

SAS-3 Operations

The SAS-3 observatory is operated from the

Multisat Center at NASA/GSFC by controllers who implement the requests of the scientific observers at M.I.T. The observers' requests are telephoned from the SAS-3 data center at M.I.T. to NASA/GSFC at least 30 min before each pass over a ground station. Tape-recorded playback data of every other orbit are transmitted to M.I.T. via an open data line and processed for preliminary scientific evaluation and operational planning within about an hour after their original receipt at the tracking station. The preliminary analysis allows the scientists at M.I.T. to determine the status of the experiment and spacecraft and to evaluate the quality of the data from the current observation. Commands to correct the spin-axis direction (using the Z-axis trim system) and the attitude of the satellite about the spin axis (by means of the commandable rate gyro of the azimuthal control system) are sent to NASA/GSFC in time for the next pass over a ground station (about 100 minutes later). The desired attitude of the X-ray detectors on the experiment can thereby be maintained to within about ± 10 arc-minutes for the duration of a given observation, typically a few days.

The actual operation of the satellite is controlled by the two on-board Delayed Command Subsystems (DCS). For each observation, an optimum set of up to 15 commands for each orbit is determined by the scientist. This sequence of commands, with specified delays, is loaded into both of the DCS's. The set of commands in a DCS is initiated by an "epoch set" command sent in real time from a ground station or by the other DCS. This feature permits the observatory to be operated with both DCS's loaded with a group of commands appropriate to a given observation, and with the last command in each DCS being an "epoch set" for the other DCS. The DCS's then cycle alternately and automatically with the precision of the on-board clock.

A sequence of operations can thus be established that is synchronized with the orbital period and designed to use optimally all portions of each orbit. For example, two X-ray sources are commonly observed during each orbit. Using the DCS and the commandable rate gyro system, each source is observed while the other is occulted by the earth, thus avoiding the normal 40% loss of data due to earth occultation.

The effectiveness of the DCS's, as well as of the other spacecraft systems, can be seen in the results obtained from the few selected observations described below.

Scientific Results

Vela X-1

Vela X-1 (3U0900-40) is one of eight known binary systems that emit hard (>2 keV) X rays at luminosities greater than about 10^{36} ergs s^{-1}. Discovered by means of rocket observations in 1967, it was found by OSO-7 satellite observations to be an eclipsing binary with an orbital period of approximately nine days. Refinement of positional data by the Uhuru (SAS-1) satellite observations led to identification of its optical counterpart, HD77581, a supergiant, and to determinations of the mass function for the optical star.

The SAS-3 observations began on June 18, 1975 when data recorded during a brief scan over 3U0900-40 revealed that the source was in a state of high intensity, equal to about a third that of the Crab Nebula (8 to 19 keV). The satellite was then switched from the scanning mode to the pointed mode of operation (three-axis stabilized), so that 3U0900-40 was nearly centered in the detectors' field of view throughout the portion of each satellite orbit that the source was not occulted by the earth. Each orbital period yielded about 3000 s of observations. It was immediately evident that the flux was periodic with the pulse period about 141 s (Fig. 3). However, further study revealed that there were subtle differences between even and odd pulses at higher energies ($E \gtrsim 10$ keV) and gross differences at lower energies. Hence, the correct period was deduced to be 282.9 s.

The existence of X-ray pulsations with a stable pulse period of 282.9 s allows the X-ray star's orbit to be determined from the periodic variations in the pulse arrival times. In effect, we can treat the system as a double-line "spectroscopic" binary. We "folded" the counting rate data from each of 35 satellite orbits into the 282.9-s pulse period, using all the available photon statistics to determine the arrival time of a fiducial (reference) feature on the pulse profile. We thus obtained 35 arrival times of "clock ticks" from 3U0900-40 that have a statistical uncertainty of about 5 s. Each arrival time was corrected for time delay with respect to the center of the sun.

From an initial inspection of the pulse arrival times, it was evident that a constant apparent

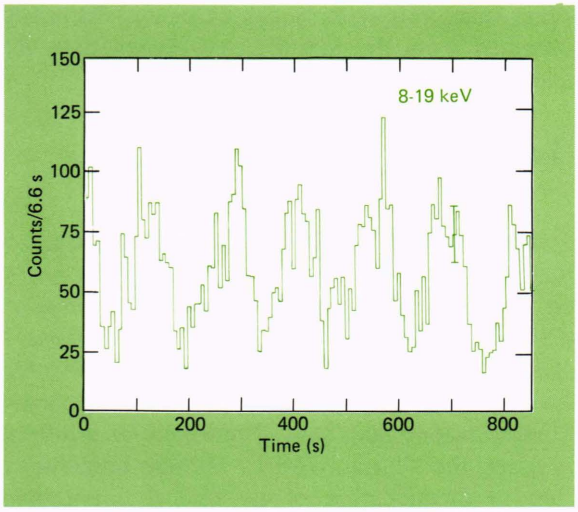

Fig. 3—Data from 3U0900-40. Raw count rate data are plotted for 15 min of observation. A background counting rate of 50 counts/6.6 s has been subtracted. SAS-3 was in a pointed mode (3-axis stabilized) while these data were obtained.

period would not fit the data. This lack of constancy results from the doppler delays as the X-ray source traverses its orbit about its companion star.

We carried out a minimum χ^2 fit of a theoretical doppler curve with orbital eccentricity to the 35 observations in June and July 1975 of pulse arrival times. (χ^2 is a statistical measure of the deviation of the observed from the expected values.) The minimum fits to circular and eccentric orbits are illustrated in Fig. 4. Open and closed circles are June and July 1975 observations, respectively; the small dots are the residuals; and the solid lines are the best-fit theoretical curves. The circular fit produces a distribution of residuals with a period of about $P_{orb}/2$ (see Fig. 4a). This systematic distribution of residuals is reduced to a random scatter and the value of χ^2_{min} is reduced by a factor of about 2 when an eccentric orbit is used (Fig. 4b). The rms scatter of the residuals for the eccentric fit is 4.0 s, which is comparable to the statistical uncertainty in the arrival time of each pulse.

If we combine the results of this analysis with similar observations of the optical companion HD77581, we obtain $M_x \gtrsim (1.45 \pm 0.16\ M_\odot)$, where $M_\odot$ is a solar mass, and $M_{opt} \gtrsim (21.1 \pm 0.9\ M_\odot$ for the masses of the X-ray and optical stars, respectively. The existence of X-ray pulsations with a highly stable pulse period rules out the possibility that the X-ray star is a black hole. Moreover, the mass of the X-ray star probably exceeds the maximum stable mass of a white dwarf.

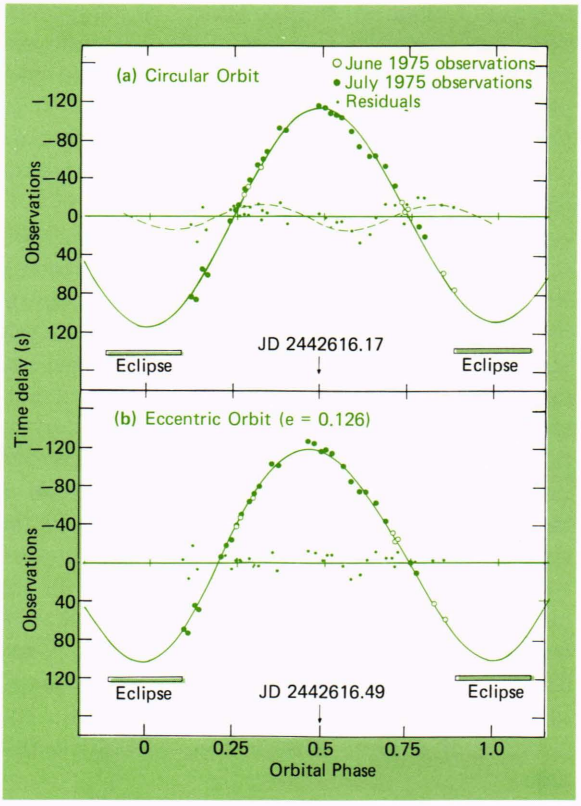

Fig. 4—Doppler shift in 3U0900-40. The doppler corrections to the pulse arrival times are plotted as a function of the 8.966-day orbital phase for (a) the best-fit circular orbit and (b) the best-fit eccentric orbit. The solid lines are the best-fit theoretical curves.

It is therefore likely that the X-ray source is an accreting neutron star.

Transient X-ray Source

During the last decade, nearly a dozen transient X-ray sources with lifetimes of days to weeks have been reported. Satellite detectors have recently recorded several transient events that lasted only for hours. Their apparent celestial positions were determined to an accuracy of a few degrees. However, the data were not sufficient to eliminate the possibility that some, perhaps all, of these events were caused by solar X rays spuriously recorded by the satellite instrumentation.

A transient source of hard X rays, designated MX2346-65, was detected by the SAS-3 satellite on November 16, 1975. At detection time, the satellite was spinning at two revolutions per 95-min orbital period, with its spin axis at a right ascension $\alpha(1950) = 40.0°$ and a declination $\delta(1950) = 13.8°$. The counting rate data from four of the collimated proportional counters are

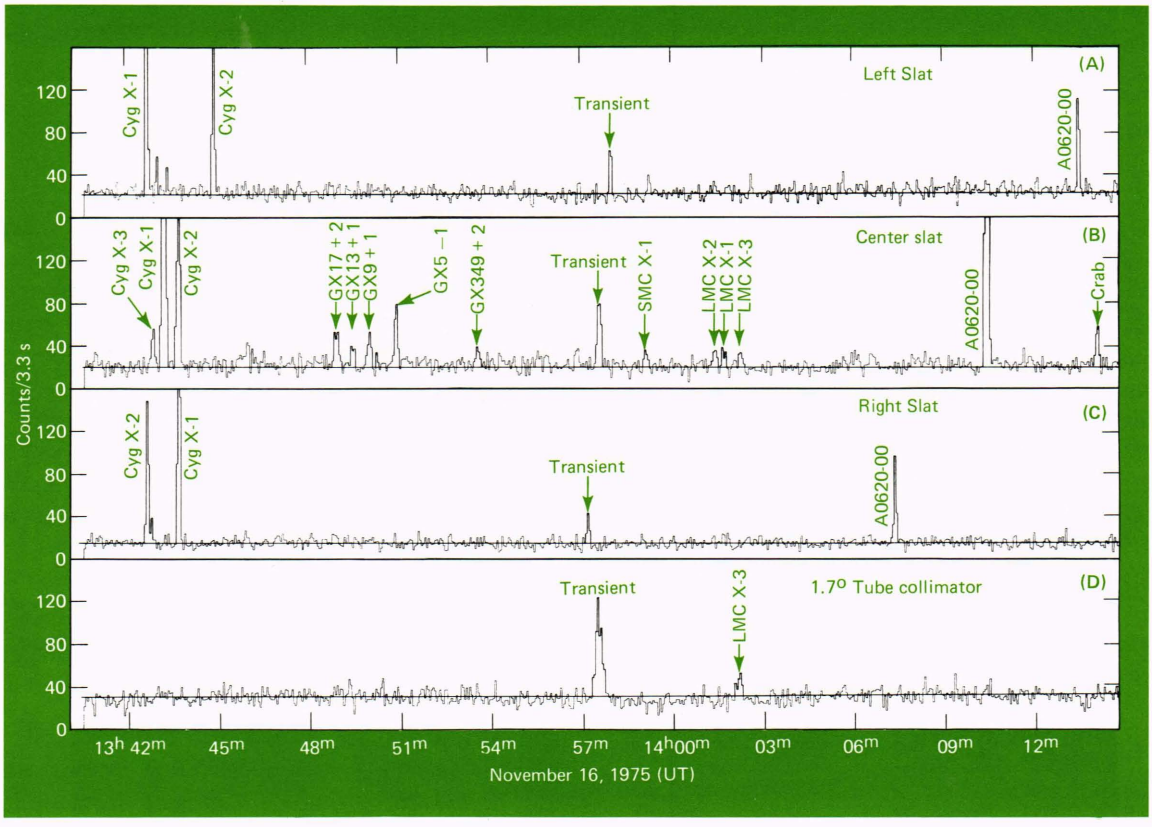

Fig. 5—Transient X-ray source. The counting rate data are plotted for four of the collimated proportional counters aboard SAS-3. The energy interval is ≈1.5 to 15 keV. The difference in time between sighting of a source in the left (a) and the right (b) slat collimators is a measure of the elevation of the source with respect to the satellite equator. The transient source detected at ≈13^h57^m is determined to be at a satellite elevation of 5.0°, which is confirmed by its detection in the inclined tube collimator (d).

shown in Fig. 5. Three of the detectors are behind slat collimators. The center slat has a $1° \times 30°$ full width half maximum (FWHM). The crossed slats have $0.5° \times 32°$ FWHM fields of view and are oriented at $\pm 30°$ with respect to the center slat. The centers of the fields of view are coaligned on the equatorial plane of the satellite. The fourth detector has a circular field of view of 1.7° FWHM that is tilted up 5° from the equatorial plane.

The counting rate data from the center slat (Fig. 5) shows the bright sources Cyg X-1, Cyg X-2, and Nova Monocerotis (A0620-00). The bright sources located near the galactic center region are visible also, though at a low counting rate since they were about 40° from the satellite equator. Sources at that elevation do not appear in the crossed slat detectors although, with low statistical significance, SMC X-1 and the three LMC sources are detected.

The transient source was detected with approximately equal peak counting rates successively in the left, center, and right slat collimators, beginning at November $16^d13^h57^m05^s$ (UT) and following at 22-s intervals, as expected for a source at an elevation of 5° above the satellite equator. From the known stability of the spacecraft clock and the gyro control system, we derive the azimuth of the source relative to that of reference sources with known positions. Since no star sensor data are available for the time of the source detection, the stability of the spacecraft clock and gyro are used to determine the orientation of the spin axis by means of the relative detection times of the identified X-ray sources. The position of the transient source obtained in this way is

$$\alpha(1950) = 23^h45^m6^s$$

$$\delta(1950) = -64°42'$$

with an 80% confidence error radius of 40′. The

calculated position of the source implies that it should be visible in the tilted-up detector; it is in fact seen with the detector (Fig. 5d).

The position of the transient source was also scanned by the satellite on November 16 at the following times: 9^h14^m, 10^h49^m, and 12^h23^m, immediately preceding the detection at 13^h57^m (UT). No source was detected down to a level of about a quarter of the intensity apparent in Fig. 5. At intermediate times, the detectors scanned over the direction of the source, but it may have been occulted by the earth. The uncertainty of the earth occultation arises solely from the approximately 1% uncertainty in the source position. The source location was also scanned every 95 min during the following seven days with no further evidence of X-ray activity.

The SAS-3 observation is especially noteworthy for the following reasons: (a) the event is clearly of celestial origin; (b) it is among the fastest reported to date (<36 min in duration); (c) the source is located at a high galactic latitude, with a comparatively accurately determined position; and (d) its energy spectrum is extremely hard.

Crab Nebula

The Crab Nebula, in the constellation Taurus, is the remnant of a supernova explosion that occurred in June 1054 A.D. Chinese and Japanese astronomers recorded the sudden appearance of this "quest star." At first it was brighter than Venus and could be seen in the daytime for several weeks. As it faded, it remained visible in the night sky for about two years. An optical photograph of the Crab Nebula shows that the object presently consists of a central mass surrounded by intertwining filaments. Its apparent size is expanding at a rate of 1% every eight years. At that angular velocity, the nebulosity would have taken about 800 years to reach its observed size from an initial point explosion. In 1928 this expansion time led to the correlation of the nebula with the 1054 supernova.

In 1964, the Crab Nebula was discovered to be a copious emitter of X rays. Scientists at the Naval Research Laboratory were able to identify the X-ray source with the nebula by means of a sounding rocket flight during which the limb of the moon occulted the X-ray source. Subsequently, high-energy X rays and gamma rays have been observed from the nebula.

The source region for 70% of the photons between 20 and 150 keV in energy is indicated by the parallelogram shown on the cover. The parallelogram is superimposed on a photo of the nebula's optical features.

The energy source of the radiation from the Crab Nebula remained a mystery until a radio pulsar with a period of about 33 ms was discovered there in 1968. Subsequent observations showed that the pulsar (NP 0532) also emits at optical and X-ray wavelengths and that it is slowing down with time. (NP 0532 is shown on the cover in a red circle for reference purposes.) It is now agreed that the pulsar is a rapidly rotating neutron star and that the emission from the Crab Nebula is powered by the rotational energy given up by the pulsar as it slows down. The mechanism for this energy transfer is still not clear. Therefore, we undertook with SAS-3 to measure the X-ray light curve (intensity versus time) using the very stable spacecraft clock to enable us to superimpose data obtained over a two-day period in May 1975.

The profile of the X-ray pulse as recorded by the SAS-3 satellite is shown in the top curve of Fig. 6. The data stream has been "folded" into the period of pulsation determined from optical data. Two peaks of X-radiation from the pulsar are seen to rise above the steadier radiation from the associated nebula. The bottom curve of Fig. 6 shows the arrival rates for optical photons. The curve has been degraded in resolution to match that of the X-ray curve above it.

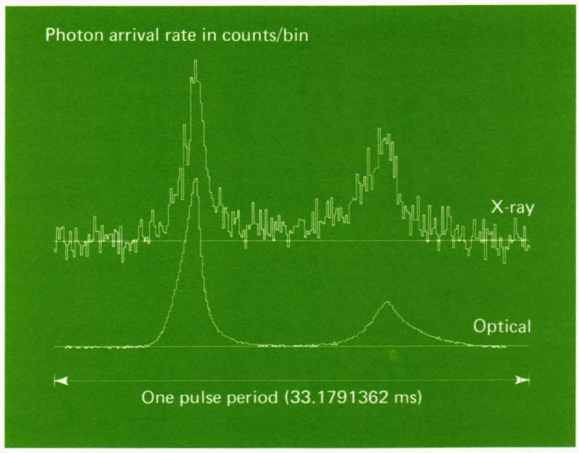

Fig. 6—Crab Nebula pulsar. The arrival rates of photons from the Crab Nebula pulsar (NP0532) are plotted against the phase of the known period of about 33 ms. The data stream has been "folded" about this period to improve the statistics of each bin. The optical curve has been degraded in resolution to match that of the X-ray curve above it.

The remarkable correlation between X-ray and optical profiles, as well as the fast rise and fall of the first pulse but the slow rise of the second, must be explained by any proposed theory of the Crab Nebula/pulsar energetics. Theoreticians are still trying to solve the problem.

Perseus Cluster of Galaxies

Since launch, the SAS-3 observatory has determined the precise positions of about 50 X-ray sources. The fundamental objective of each measurement is to identify the X-ray source with an optical or radio object so that the properties of the source can be studied over the entire electromagnetic spectrum. Such unambiguous identification requires either a correlated time variation in the intensities of the X-ray and optical objects (e.g., the nine-day eclipsing binary system of Vela X-1) or an X-ray position so precise (about 10 arc-seconds) that only one unusual object is within the error box of the X-ray source.

As mentioned earlier, position measurements are made with two modulation collimators that view the sky along the satellite spin axis. Each collimator consists of two planes of wires. The wires in each plane are 0.003 in. in diameter and 0.003 in. apart. The two planes are separated by about 2 and 4 in., respectively, in the two collimators. These dimensions yield periodic angular response functions of 4.5 and 2.3 arc-minutes, respectively. As the satellite rotates about its spin axis, the observed intensity of a point source is modulated in a manner that depends upon the position of the source in the field of view. The source position is obtained by comparing the observed modulations in the data with those that would be expected from a source at a trial position. The comparison is repeated for all points on the sky within the collimator's 12° field of view. For each trial position, a correlation value is determined that depends on the agreement between the expected and observed data. A map of the correlation values shows the position of the X-ray source.

Obviously, the analysis depends critically on knowledge of the satellite orientation at any time. However, the cameras on SAS-3 can measure the position of only one star at a time. Thus, we rely on the stability of the spacecraft motion to allow us to superimpose successive star sightings to obtain, in effect, a picture of the star field and thereby to determine the satellite orientation. The stability of the spacecraft motion, which is determined by the gyro control system and the nutation damper on the APL spacecraft, has proven to be a factor of 10 better than requested. At present, we have attained the 10-arc-second goal and, in light of the performance of the gyro and nutation damper, expect to reduce even further the uncertainty in the aspect determination.

The observation of the Perseus cluster of galaxies represents a typical measurement of X-ray source positions. The cluster had first been observed by SAS-1 and OSO-7 to emit X rays and more recently by the Copernicus satellite (OAO-C). However, the resolution of the earlier measurements was insufficient to determine whether the X rays were emitted by one or more of the individual galaxies or possibly even by the region between galaxies.

Data from the Perseus cluster were obtained from October 21, to November 1, 1975 by a SAS-3 co-investigator who is now at the Smithsonian Astrophysical Observatory. The correlation map of the region is shown in Fig. 7. A point source appears as a bright spot surrounded by a series of rings. The Perseus cluster is at the left center of the picture. The position determined by SAS-3 places the X-ray source on a bright exploding radio galaxy, NGC1275, near the middle of the cluster. No X rays were detected from other galaxies in the cluster, nor from the regions between the galaxies.

Figure 7 also shows another, previously unreported, X-ray source at the right center of the picture. The position determined for this source is within 10 arc-seconds of the triple star system of Algol (β Persei), which is a bright, flaring, radio source. Thus, one observation has resulted in the confirmation of one source and the discovery and identification of another.

Vela Supernova Remnant

A final example of the use of the spacecraft's capabilities to perform complicated scientific measurements is the observation of the Vela supernova remnant (Vela SNR). Analysis of the data obtained during the observation is continuing. However, the techniques used to make the observation probably represent the ultimate use of the spacecraft and therefore should be described.

The Vela SNR is quite similar to the Crab Nebula in that a past supernova explosion left a

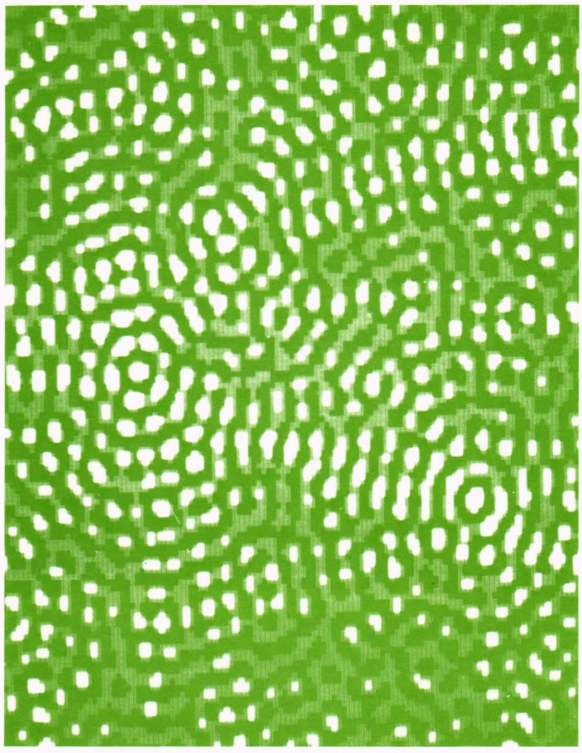

Fig. 7—Correlation map of the Perseus cluster. The correlation values, quantized into three levels, are plotted for each point in the 12° field of the 4.5-arc-minute modulation collimator. A point source appears as a bright spot surrounded by rings of decreasing intensity. The diameter of the first ring about a source is 18-arc-minutes. The source to the left-center of the map is NGC1275; that to the right and slightly below center is Algol (β Persei).

gaseous nebulosity, and a pulsar near the center supplies the energy for the observed radiation. However, the supernova in Vela is estimated to have occurred about 13,000 years ago. Since the explosion, the source has been expanding so that it presently has an angular diameter of about 5° to 6°. The goal of the SAS-3 observation was to obtain a two-dimensional spatial profile, i.e., an X-ray picture of the source.

To obtain the picture, we used a detector system sensitive to very-low energy X rays (0.15 to 1.0 keV) that views the sky with a 1° circular field of view in the equatorial plane of the satellite. The spin axis position for the observation was chosen so that, by using the spin axis trim system, a deliberate drift of the spin axis could be introduced that would result in a detector motion perpendicular to the one introduced by a scanning motion (dither back and forth) about the spin axis. Thus, by means of three systems—the delayed command, spin axis trim, and azimuthal control—we were able to execute a slow raster scan over the entire Vela SNR. The drift rate of the spin axis was adjusted so that each line of the raster was displaced from the preceding line by about 0.5° (half the beam size of the detector system). Each orbit produced a new line in the raster scan.

The raw line-scan data obtained over a period of several days were combined with the known angular response curve of the detector system to produce the X-ray picture shown in Fig. 8. It is a two-dimensional intensity contour map of the Vela SNR region in celestial coordinates. Three "hot spots" can be seen, but none is correlated with the PSR 0833-45 pulsar.

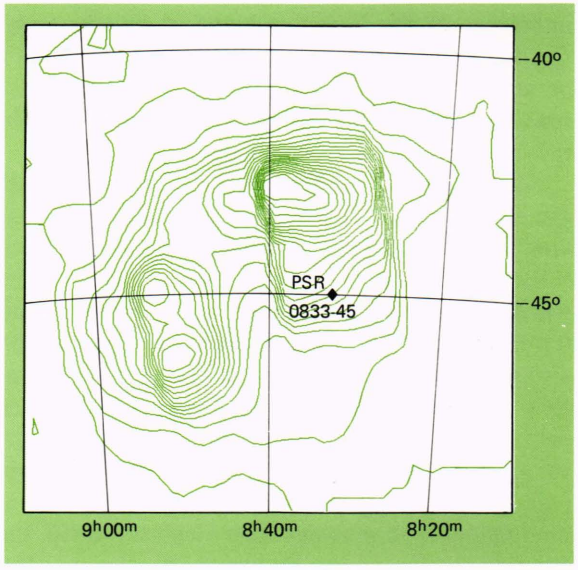

Fig. 8—Low-energy map of the Vela SNR. The X-ray flux in the energy interval 0.15 to 1.0 keV is plotted versus position in the Vela supernova remnant. This contour map is obtained by deconvolving data obtained in a line raster scan over the source. No X rays were detected from the pulsar PSR 0833-45.

Conclusion

The APL SAS-3 spacecraft provides the sophistication and flexibility that enable the scientists at M.I.T. to use it as a true observatory. Moreover, we are pleased that we have effectively used every improvement incorporated into the spacecraft.

Although this review emphasizes the systems unique to SAS-3, the successful results described herein depend on many systems that are not discussed but that performed excellently during the first year of operation.